# Supplementary Materials for "On Functional Processes with Multiple Discontinuities"

Jialiang Li*
Department of Statistics and Applied Probability
National University of Singapore

Yaguang Li
School of Management, University of Science and Technology of China

Tailen Hsing
Department of Statistics, University of Michigan, USA

## 1 Additional results from simulation study

In this section, we provide more simulation results. The following part includes the Gaussian and the heavy tailed cases with sample size $n = 100, m = 100$, and $n = 50, m = 300$.

### 1.1 Simulation 1

Consider the same mean function settings as in the main paper:

- Setting 1: $\mu(t) = \sin(2\pi t) + \cos(2\pi t) + t^2 + \sum_{k=1}^{3} d_k I(t \geq \tau_k)$,

*Email:stalj@nus.edu.sg

with $M = 3$ change points at $(\tau_1, \tau_2, \tau_3) = (0.25, 0.5, 0.75)$ and jump sizes $(d_1, d_2, d_3) = (0.5, -0.4, 0.4)$, and

- Setting 2: $\mu(t) = \sin(2\pi t) + \sum_{k=1}^{5} d_k I(t \geq \tau_k)$,

with $M = 5$ change points at $(\tau_1, \tau_2, \tau_3, \tau_4, \tau_5) = (0.167, 0.333, 0.500, 0.667, 0.833)$ and jump sizes $(d_1, d_2, d_3, d_4, d_5) = (0.45, -0.5, 0.45, -0.5, 0.45)$. The true covariance function is designed as

$$R(s,t) = \sum_{k=1}^{3} \xi_k \psi_k(s)\psi_k(t), \qquad s, t \in [0,1],$$

where $\xi_k = 1/(k+1)^2,\ k = 1, 2, 3$, and

$$\psi_1(t) = 1, \qquad \psi_2(t) = \sqrt{2}\sin(2\pi t), \qquad \psi_3(t) = \sqrt{2}\cos(2\pi t).$$

The data are then generated from model (1) with $T_{ij} \sim \text{Uniform}[0,1]$, $U_{ij} = \sum_{k=1}^{3} a_{ik}\psi_k(T_{ij})$ where $a_{ik}$ are independent from $N(0, \xi_k)$ and $e_{ij} \sim N(0, 0.2^2)$.

In addition to the cases considered in the main paper, we consider another setting with $n = 100, m = 100$, and $n = 50, m = 300$, where $m_i \sim \text{Poisson}(m)$ for different settings, which stands for a purely ultra-dense functional data with small $n$.

Tables 1–2 present the performance of the proposed change point detection procedure for the case $n = 100, m = 100$, and $n = 50, m = 300$. Observe that the performance improves as the $m_i$ increases. The MISEs are reported in Table 3.

Furthermore, Figure 1 displays representative smoothed mean estimation after consistently detecting the change point in three settings along with the 95% confidence band constructed from asymptotic normal approximation. The selected curve estimation corresponds to the case with median MISE among the $L$ simulations. Similar as $n = 400$ case, the estimation accuracy improves when $m_i$ increases.

## 1.2 Simulation 2

We next generate data assuming a heavy-tailed process to illustrate the applicability of our proposed methods. We consider the same true mean and covariance function

Table 1: Performance of change point detection for setting 1 in simulation 1. The corresponding standard deviations are in the parentheses.

| | | $n = 100$, $m = 100$ | $n = 50$, $m = 300$ |
|---|---|---|---|
| SUBJ | $\text{Mean}(\widehat{M}) - M$ | -0.010 | -0.075 |
| | $\text{Med}(\widehat{M}) - M$ | 0 | 0 |
| | $\mathcal{E}(\widehat{M} = M)[\%]$ | 85.0 | 92.5 |
| | $\max_i \min_j \lvert\tau_i - \widehat{\tau}_j\rvert$ | 0.0138 (0.0463) | 0.0001 (0.0001) |
| | $\max_j \min_i \lvert\tau_i - \widehat{\tau}_j\rvert$ | 0.0263 (0.0904) | 0.0188 (0.0666) |
| | $\max_k \lvert\widehat{d}_k - d_k\rvert$ | 0.1276 (0.0916) | 0.1055 (0.0395) |
| OBS | $\text{Mean}(\widehat{M}) - M$ | -0.020 | 0.010 |
| | $\text{Med}(\widehat{M}) - M$ | 0 | 0 |
| | $\mathcal{E}(\widehat{M} = M)[\%]$ | 92.0 | 95.0 |
| | $\max_i \min_j \lvert\tau_i - \widehat{\tau}_j\rvert$ | 0.0063 (0.0291) | 0.0030 (0.0189) |
| | $\max_j \min_i \lvert\tau_i - \widehat{\tau}_j\rvert$ | 0.0156 (0.0597) | 0.0063 (0.0395) |
| | $\max_k \lvert\widehat{d}_k - d_k\rvert$ | 0.1322 (0.0823) | 0.0862 (0.0371) |
| MIX | $\text{Mean}(\widehat{M}) - M$ | -0.030 | -0.045 |
| | $\text{Med}(\widehat{M}) - M$ | 0 | 0 |
| | $\mathcal{E}(\widehat{M} = M)[\%]$ | 94.0 | 95.5 |
| | $\max_i \min_j \lvert\tau_i - \widehat{\tau}_j\rvert$ | 0.0046 (0.0221) | 0.0001 (0.0001) |
| | $\max_j \min_i \lvert\tau_i - \widehat{\tau}_j\rvert$ | 0.0159 (0.0695) | 0.0113 (0.0519) |
| | $\max_k \lvert\widehat{d}_k - d_k\rvert$ | 0.1434 (0.1148) | 0.0957 (0.0385) |

settings given in the preceding subsection, except that, the data are generated from model (1) where $T_{ij} \sim \text{Uniform}[0, 1]$, $U_{ij} = \sum_{k=1}^{3} a_{ik}\psi_k(T_{ij})$, $a_{ik}$ are independent from $t$-distributed with 3 degree of freedom and $e_{ij}$ follows a $t$-distribution with 3 degree of freedom and variance 0.03.

Eyeballing Tables 4–5, we note that the accuracy of change point detection is increasing as the observations become denser. Similarly, examining Tables 6, the MISE for $\widehat{\mu}$ suggest good overall performance of our proposed estimator.

Table 2: Performance of change point detection for setting 2 in simulation 1. The corresponding standard deviations are in the parentheses.

| | | $n = 100$, $m = 100$ | $n = 50$, $m = 300$ |
|---|---|---|---|
| SUBJ | Mean$(\widehat{M}) - M$ | 0.010 | -0.020 |
| | Med$(\widehat{M}) - M$ | 0 | 0 |
| | $\mathcal{E}(\widehat{M} = M)[\%]$ | 98.5 | 96.0 |
| | $\max_i \min_j \lvert\tau_i - \widehat{\tau}_j\rvert$ | 0.0014 (0.0085) | 0.0014 (0.0115) |
| | $\max_j \min_i \lvert\tau_i - \widehat{\tau}_j\rvert$ | 0.0007 (0.0050) | 0.0057 (0.0297) |
| | $\max_k \lvert\widehat{d}_k - d_k\rvert$ | 0.1243 (0.0427) | 0.1095 (0.0421) |
| OBS | Mean$(\widehat{M}) - M$ | -0.020 | -0.020 |
| | Med$(\widehat{M}) - M$ | 0 | 0 |
| | $\mathcal{E}(\widehat{M} = M)[\%]$ | 98.0 | 98.0 |
| | $\max_i \min_j \lvert\tau_i - \widehat{\tau}_j\rvert$ | 0.0005 (0.0031) | 0.0001 (0.0001) |
| | $\max_j \min_i \lvert\tau_i - \widehat{\tau}_j\rvert$ | 0.0038 (0.0233) | 0.0032 (0.0227) |
| | $\max_k \lvert\widehat{d}_k - d_k\rvert$ | 0.1291 (0.0753) | 0.1046 (0.0366) |
| MIX | Mean$(\widehat{M}) - M$ | -0.030 | 0.015 |
| | Med$(\widehat{M}) - M$ | 0 | 0 |
| | $\mathcal{E}(\widehat{M} = M)[\%]$ | 97.0 | 97.0 |
| | $\max_i \min_j \lvert\tau_i - \widehat{\tau}_j\rvert$ | 0.0009 (0.0070) | 0.0019 (0.0130) |
| | $\max_j \min_i \lvert\tau_i - \widehat{\tau}_j\rvert$ | 0.0066 (0.0314) | 0.0016 (0.0159) |
| | $\max_k \lvert\widehat{d}_k - d_k\rvert$ | 0.1300 (0.0867) | 0.1026 (0.0378) |

Again, Figure 2 displays representative smoothed mean estimation after consistently detecting the change point along with the 95% confidence band constructed from asymptotic normal approximation. The estimated variances are somehow more diverging due to the heavy tailed distribution. In general, as $n$ or $m_i$ increases the estimation accuracy improves.

Table 3: MISE ($\times 10^{-2}$) of $\widehat{\mu}_{obs}$, $\widehat{\mu}_{subj}$ and $\widehat{\mu}_{\alpha}$ in Simulation 1. The corresponding standard deviations are in the parentheses.

| (n,m) | | $(n=50, m=300)$ | $(n=100, m=100)$ |
|---|---|---|---|
| Setting 1 | $\widehat{\mu}_{obs}$ | 0.0715 (0.0002) | 0.1064 (0.0436) |
| | $\widehat{\mu}_{obs}^{ZW}$ | 0.2699 (0.0225) | 0.3068 (0.0412) |
| | $\widehat{\mu}_{subj}$ | 0.0835 (0.0332) | 0.1174 (0.0548) |
| | $\widehat{\mu}_{subj}^{ZW}$ | 0.2679 (0.0291) | 0.3104 (0.0454) |
| | $\widehat{\mu}_{\alpha}$ | 0.0712 (0.0303) | 0.1082 (0.0484) |
| | $\widehat{\mu}_{\alpha}^{ZW}$ | 0.2668 (0.0247) | 0.3073 (0.0410) |
| Setting 2 | $\widehat{\mu}_{obs}$ | 0.0768 (0.0288) | 0.1021 (0.0376) |
| | $\widehat{\mu}_{obs}^{ZW}$ | 0.3244 (0.0421) | 0.4517 (0.0544) |
| | $\widehat{\mu}_{subj}$ | 0.0784 (0.0275) | 0.1020 (0.0344) |
| | $\widehat{\mu}_{subj}^{ZW}$ | 0.3245 (0.0422) | 0.4446 (0.0551) |
| | $\widehat{\mu}_{\alpha}$ | 0.0732 (0.0275) | 0.1114 (0.0388) |
| | $\widehat{\mu}_{\alpha}^{ZW}$ | 0.3248 (0.0422) | 0.4524 (0.0599) |

# 2 Additional case studies

## 2.1 Australian Temperature Data

Australian daily minimum temperature climate data form year 1855 to 2012 for 8 different stations are investigated in Aue et al. (2018). The stations that the daily temperature data is taken are: Sydney (Observatory Hill), Melbourne (Regional Office), Boulia Airport, Cape Otway Lighthouse, Gayndah Post Office, Gunnedah Pool, Hobart (Ellerslie Road), Robe Comparison. The data is taken from Australian Government Bureau of Meteorology. The daily observations are available from `http://www.bom.gov.au/climate/data`. Copyright Commonwealth of Australia 2010, Bureau of Meteorology. The data is available in the `R` package `fChange`. Definitions of variables are adapted from `http://www.bom.gov.au/climate/dwo/IDCJDW0000.shtml`.

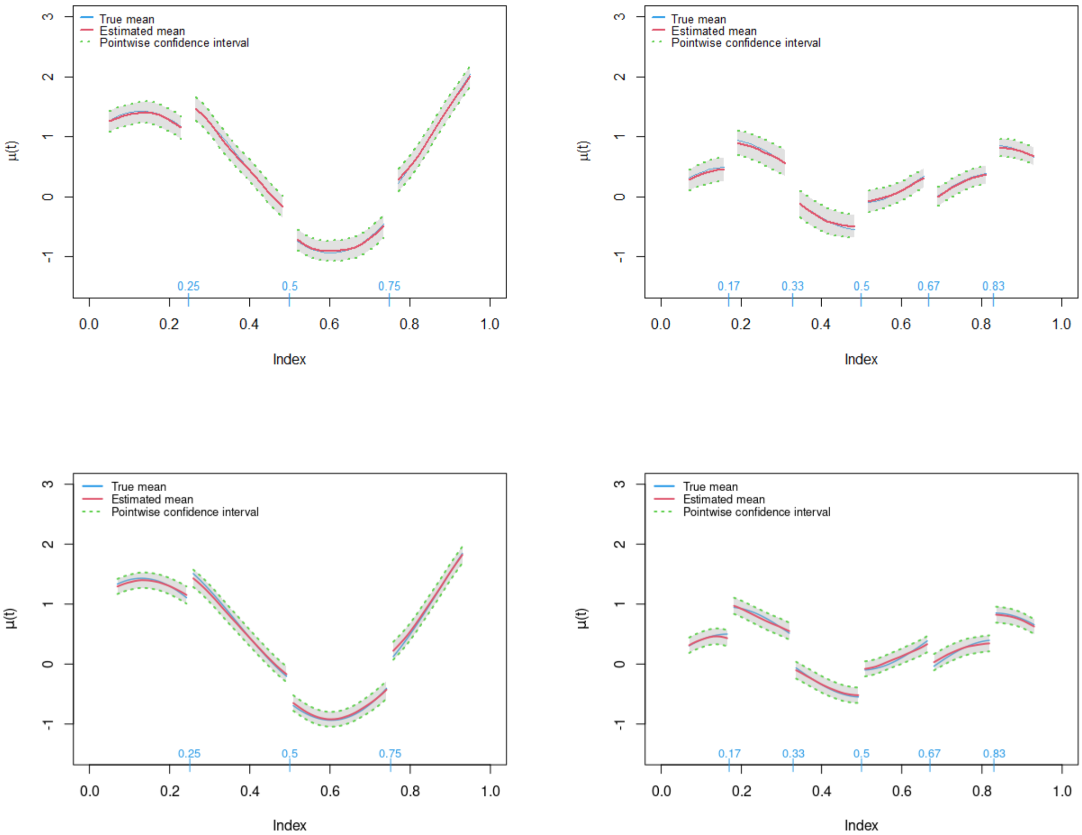


Figure 1: Smoothed mean function estimation and 95% confidence band from asymptotic normal approximation with the mixture weight. The two columns correspond to setting 1 and setting 2, and the two rows correspond to $m = 100, 300$, respectively.

We take the Sydney station data as an example to illustrate our method. Based on the work of Aue et al. (2018), a subset is extracted which we can assume that the data follow an identical distribution. The extracted dataset consists of $m_i = 365$ (366 in leap years) daily measurements of minimum temperatures from year 1957 to 2011 ($n = 55$) . We then apply our method to estimate the mean curve for daily minimum temperature for this station. From Figure 3, 2 jumps are detected at July 5 and October 26 of an average year. The estimated jump sizes at the five points are $-0.809$ and 0.630, respectively. The overall mean curve thus displays four smoothing segments, indicating sudden changes in different seasons. Also, to

Table 4: Performance of change point detection for setting 1 in simulation 2. The corresponding standard deviations are in the parentheses.

| | | $n = 100$, $m = 100$ | $n = 50$, $m = 300$ |
|---|---|---|---|
| SUBJ | $\text{Mean}(\widehat{M}) - M$ | 0.020 | -0.030 |
| | $\text{Med}(\widehat{M}) - M$ | 0 | 0 |
| | $\mathcal{E}(\widehat{M} = M)[\%]$ | 84.0 | 97.0 |
| | $\max_i \min_j \lvert\tau_i - \widehat{\tau}_j\rvert$ | 0.0124 (0.0395) | 0.0001 (0.0001) |
| | $\max_j \min_i \lvert\tau_i - \widehat{\tau}_j\rvert$ | 0.0284 (0.0934) | 0.0075 (0.0427) |
| | $\max_k \lvert\widehat{d}_k - d_k\rvert$ | 0.1136 (0.0422) | 0.0960 (0.0446) |
| OBS | $\text{Mean}(\widehat{M}) - M$ | 0.020 | -0.021 |
| | $\text{Med}(\widehat{M}) - M$ | 0 | 0 |
| | $\mathcal{E}(\widehat{M} = M)[\%]$ | 85.0 | 98.0 |
| | $\max_i \min_j \lvert\tau_i - \widehat{\tau}_j\rvert$ | 0.0157 (0.0481) | 0.0001 (0.0001) |
| | $\max_j \min_i \lvert\tau_i - \widehat{\tau}_j\rvert$ | 0.0173 (0.0630) | 0.0053 (0.0361) |
| | $\max_k \lvert\widehat{d}_k - d_k\rvert$ | 0.1140 (0.0793) | 0.0970 (0.0392) |
| MIX | $\text{Mean}(\widehat{M}) - M$ | -0.120 | -0.065 |
| | $\text{Med}(\widehat{M}) - M$ | 0 | 0 |
| | $\mathcal{E}(\widehat{M} = M)[\%]$ | 89.0 | 91.5 |
| | $\max_i \min_j \lvert\tau_i - \widehat{\tau}_j\rvert$ | 0.0071 (0.0296) | 0.0019 (0.0153) |
| | $\max_j \min_i \lvert\tau_i - \widehat{\tau}_j\rvert$ | 0.0421 (0.0989) | 0.0200 (0.0678) |
| | $\max_k \lvert\widehat{d}_k - d_k\rvert$ | 0.1365 (0.1422) | 0.1047 (0.0718) |

compare the individual estimate, we estimate the individual functions using the two methods described for the preceding example. We select 9 latest years and show their estimates in Figure 4. We make similar observations as the previous examples.

# References

Aue, A., G. Rice, and O. Sönmez (2018). Detecting and dating structural breaks in functional data without dimension reduction. *Journal of the Royal Statistical*

Table 5: Performance of change point detection for setting 2 in simulation 2. The corresponding standard deviations are in the parentheses.

| | | $\boldsymbol{n = 100}$, $\boldsymbol{m = 100}$ | $\boldsymbol{n = 50}$, $\boldsymbol{m = 300}$ |
|---|---|---|---|
| SUBJ | $\text{Mean}(\widehat{M}) - M$ | -0.030 | -0.010 |
| | $\text{Med}(\widehat{M}) - M$ | 0 | 0 |
| | $\mathcal{E}(\widehat{M} = M)[\%]$ | 97.0 | 96.5 |
| | $\max_i \min_j \lvert\tau_i - \widehat{\tau}_j\rvert$ | 0.0006 (0.0021) | 0.0019 (0.0136) |
| | $\max_j \min_i \lvert\tau_i - \widehat{\tau}_j\rvert$ | 0.0054 (0.0274) | 0.0041 (0.0253) |
| | $\max_k \lvert\widehat{d}_k - d_k\rvert$ | 0.1236 (0.0437) | 0.1049 (0.0682) |
| OBS | $\text{Mean}(\widehat{M}) - M$ | -0.010 | -0.005 |
| | $\text{Med}(\widehat{M}) - M$ | 0 | 0 |
| | $\mathcal{E}(\widehat{M} = M)[\%]$ | 97.0 | 96.5 |
| | $\max_i \min_j \lvert\tau_i - \widehat{\tau}_j\rvert$ | 0.0012 (0.0084) | 0.0019 (0.0136) |
| | $\max_j \min_i \lvert\tau_i - \widehat{\tau}_j\rvert$ | 0.0036 (0.0226) | 0.0041 (0.0253) |
| | $\max_k \lvert\widehat{d}_k - d_k\rvert$ | 0.1126 (0.0716) | 0.1050 (0.0681) |
| MIX | $\text{Mean}(\widehat{M}) - M$ | -0.045 | -0.015 |
| | $\text{Med}(\widehat{M}) - M$ | 0 | 0 |
| | $\mathcal{E}(\widehat{M} = M)[\%]$ | 94.5 | 98.0 |
| | $\max_i \min_j \lvert\tau_i - \widehat{\tau}_j\rvert$ | 0.0014 (0.0113) | 0.0011 (0.0110) |
| | $\max_j \min_i \lvert\tau_i - \widehat{\tau}_j\rvert$ | 0.0093 (0.0473) | 0.0028 (0.0204) |
| | $\max_k \lvert\widehat{d}_k - d_k\rvert$ | 0.1182 (0.0622) | 0.1056 (0.0546) |

*Society: Series B (Statistical Methodology) 80*(3), 509–529.

Xia, Z. and P. Qiu (2015). Jump information criterion for statistical inference in estimating discontinuous curves. *Biometrika 102*(2), 397–408.

Table 6: MISE ($\times 10^{-2}$) of $\widehat{\mu}_{obs}$, $\widehat{\mu}_{subj}$ and $\widehat{\mu}_{\alpha}$ in Simulation 2. The corresponding standard deviations are in the parentheses.

| (n,m) | | $(n = 50, m = 300)$ | $(n = 100, m = 100)$ |
|---|---|---|---|
| Setting 1 | $\widehat{\mu}_{obs}$ | 0.0755 (0.0311) | 0.1008 (0.0387) |
| | $\widehat{\mu}_{obs}^{ZW}$ | 0.2638 (0.0231) | 0.3008 (0.0380) |
| | $\widehat{\mu}_{subj}$ | 0.0682 (0.0292) | 0.1080 (0.0475) |
| | $\widehat{\mu}_{subj}^{ZW}$ | 0.2650 (0.0255) | 0.3064 (0.0425) |
| | $\widehat{\mu}_{\alpha}$ | 0.0738 (0.0323) | 0.1121 (0.0536) |
| | $\widehat{\mu}_{\alpha}^{ZW}$ | 0.2641 (0.0256) | 0.3107 (0.0357) |
| Setting 2 | $\widehat{\mu}_{obs}$ | 0.0737 (0.0276) | 0.0986 (0.0380) |
| | $\widehat{\mu}_{obs}^{ZW}$ | 0.3222 (0.0476) | 0.4398 (0.0602) |
| | $\widehat{\mu}_{subj}$ | 0.0738 (0.0277) | 0.1081 (0.0524) |
| | $\widehat{\mu}_{subj}^{ZW}$ | 0.3221 (0.0477) | 0.4379 (0.0655) |
| | $\widehat{\mu}_{\alpha}$ | 0.0715 (0.0297) | 0.1042 (0.0539) |
| | $\widehat{\mu}_{\alpha}^{ZW}$ | 0.3227 (0.0428) | 0.4347 (0.0606) |

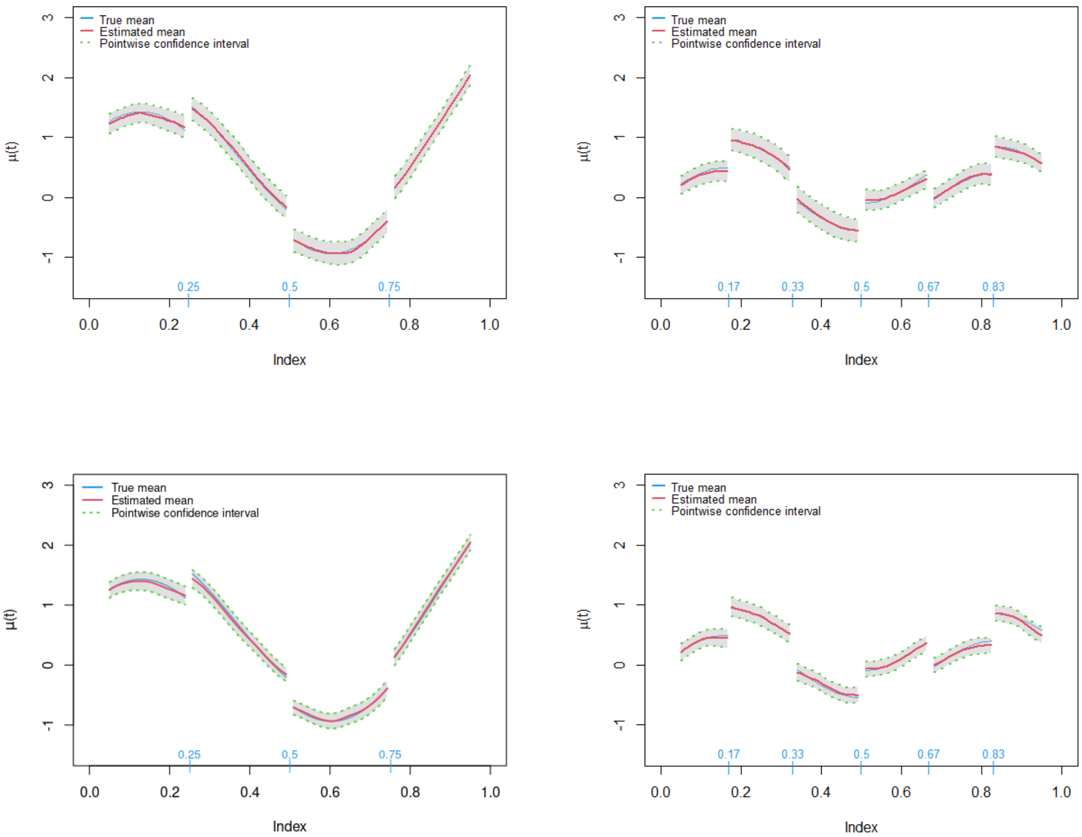


Figure 2: Smoothed mean function estimation and 95% confidence band from asymptotic normal approximation with the mixture weight. The two columns correspond to setting 1 and setting 2, and the two rows correspond to $m = 100, 300$, respectively.

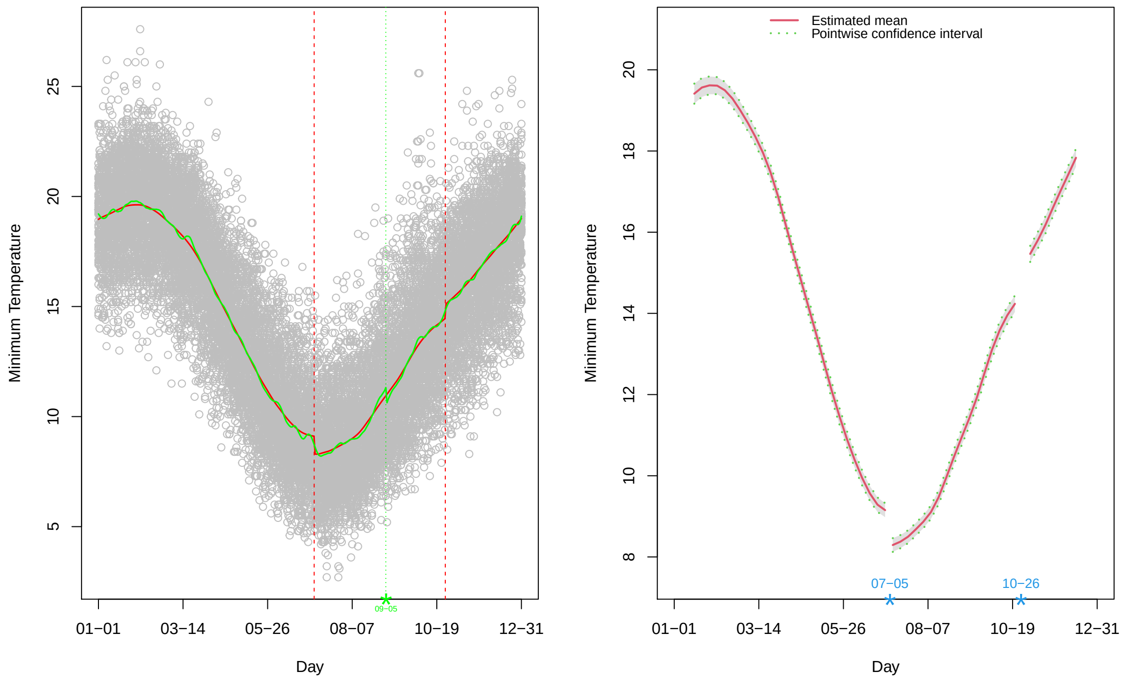


Figure 3: Mean curve of the Sydney Temperature (Degree C) for the period 1957-2011. Left panel: The red solid line is the mean function estimate $\hat{\mu}(t)$, the vertical dash lines show the change point locations, the green curve is the estimate using Xia and Qiu (2015). Right panel: Smoothed mean function estimation and 95% confidence band from asymptotic normal.

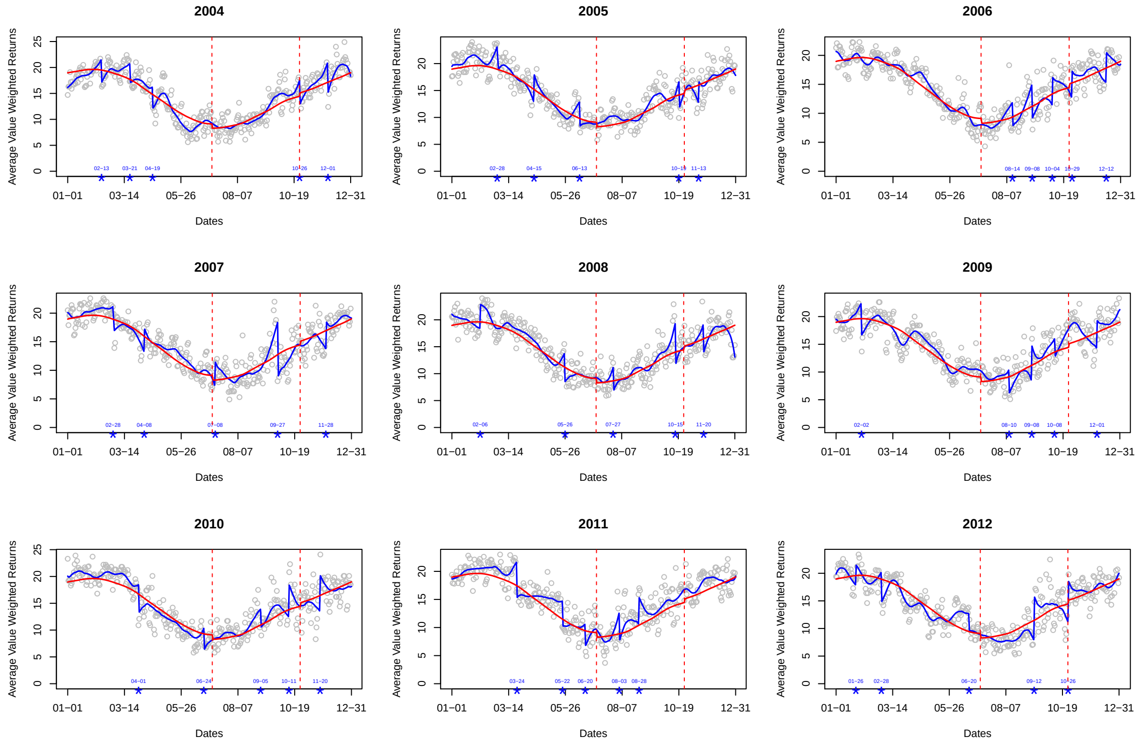


Figure 4: Individual mean curve of the Sydney temp for the period 2004-2012. The blue curve is the individual estimate and the red curve is $\hat{\mu}(t)$ using our approach.